



A New Distinctive Methodology for the Classification of Brain MR Images Using Histogram Based Local Feature Descriptors

K.Sowjanya¹, K.Rasool Reddy² and M.Raveena³

¹Department of ECE, Kakatiya Institute of Technology Science, Warangal, India-506015

²Department of ECE, Malla Reddy College of Engineering and Technology, Secunderabad, India-500100

³Department of ECE, Kakatiya Institute of Technology Science, Warangal, India-506015

Received 9 Jul. 2022, Revised 10 Apr. 2023, Accepted 6 May. 2023, Published 30 May. 2023

Abstract: Brain tumors can develop at any brain location with uneven boundaries and shapes. Typically, they increased rapidly due to their size doubling in twenty-five days. If they were unrecognized in earlier phases, patients suffered from various medical problems, including death. Therefore, the identification of brain tumors in the earlier stages is one of the critical aspects. In addition, an effective imaging sequence also plays a vital role in tumor diagnosis. Magnetic resonance (MR) imaging is widely used among the available scanning approaches. Therefore, in this article, we develop a distinctive novel method to classify MR-based brain images. Here, initially, we improve the brightness of brain MR images using a median filter, and then we employ image data augmentation to increase the model's accuracy. Later, we obtain the region of interest (ROI) by Otsu's thresholding and morphological operations. Then, we extracted relevant local textures and shaped informative features from the ROI using Enhanced gradient local binary patterns (EGLBPs) and Modified pyramid histogram of oriented gradients (MPHOG). Finally, we perform classification using various supervised learning approaches: support vector machine (SVM), K-nearest neighbors (KNN), and ensemble learning. All these experiments are implemented on Harvard Medical School (HMS) database. Based on the simulation results, our proposed imaging system outperformed state-of-the-art methods in classification and segmentation. Hence, our suggested framework can be used as a predictive tool for diagnosing patients with brain tumors.

Keywords: Brain Tumors, MRI, GLBP, ROI, and Supervised Learning Approaches.

1. INTRODUCTION

Currently, scientists and researchers have been exploring the importance of image processing in various fields, including medicine, engineering, and science. Indeed, in medicine, image processing has become very significant and plays a crucial role in clinical diagnosis applications, particularly in detecting and classifying human brain-related disorders.

Brain disorders are one of the leading causes of mortality in various categories of people. Several brain disorders include cerebrovascular, neoplastic, degenerative, and inflammatory diseases. Neoplastic diseases (glioma, meningioma, and sarcoma brain tumors) frequently occur in children and adolescents (younger adults). This type of disease can cause severe complications in the brain and may lead to death if they are not recognized well in the initial phases. Thus, detecting brain tumors early is one of the most significant factors in medicine [1]. To achieve this, in this work, we have developed a unique novel system for accurate prediction, which helps physicians analyze brain tumors.

Medical imaging sequences also play a pivotal role in

developing an effective system. Therefore, we used the magnetic resonance (MR) imaging sequence in this work because it provides crucial details or information about the soft tissue and produces high-resolution images compared to the other scanning approaches [2]. Moreover, it is a noninvasive imaging sequence because it provokes multiple images of the same tissue with different contrast visualizations and other image procurement (or acquisition) protocols. These multiple imaging sequences lead to additional significant soft tissue details that help physicians accurately identify tumors.

The primary goal of this method is to design and evaluate a unique system using MR images to distinguish between normal and abnormal patients without human intervention. Hence, with this system, we can minimize the interpretation time.

The rest of the work is organized as follows: Section 2 explores the various existing approaches. Section 3 discusses the proposed technique, including tumor segmentation, feature extraction, and classification. Section 4 analyzes the segmentation and classification outcomes



of both the proposed and existing approaches. Section 5 reports discussions of the suggested methodology, and finally, Section 6 describes the conclusion of the proposed method.

2. RELATED WORK

Many recent studies have been conducted on recognizing and classifying brain MR images. This section discusses and highlights a few recent works.

Work in [3] implemented an automated approach to detect brain tumors from MR images. With this process, they achieved an accuracy of 98.17%. In [4], a novel method was developed by moment invariant (MI) and single-layer neural networks (SLN) to classify brain MR images. Using this technique, the authors obtained 98.25% classification accuracy. In [5], proposed a novel approach based on support vector machine (SVM) and Berkeley wavelet transform (BWT) for tumor identification. By such a method, they attained 96.51% accuracy. In [6], a hybrid approach was implemented using the discrete wavelet transform (DWT), principal component analysis (PCA), and a back-propagation neural network (BPNN). In this study, they achieved an accuracy of 98.29%.

Work in [7] developed a novel technique based on wavelets and SVM. With this approach, the authors attained 97.15% accuracy. A computer-aided system based on threshold-based region optimization (TBRO) and massively parallel key-point detection, and description (MP-KDD) methods are implemented to enhance classification accuracy [8]. Through this work, they obtained an accuracy of 96.57%. A study in [9] developed a new computer-aided technique using wavelet energy and kernel-based extreme learning machines (K-ELM). Here, they obtained 98.38% classification accuracy. In [10], implemented a new pathological identification system using fractional Fourier entropy (FRFE) and multilayer perceptron (MLP). By this approach, they attained 97.81% accuracy.

Work in [11] proposed a hybrid methodology based on DWT, PCA, and K-nearest neighbors (KNN). Here, they achieved 97.54% classification accuracy. A study in [12] developed automatic pathological detection using DWT and bat-optimized ELM (BA-ELM). With this methodology, they achieved an accuracy of 98.33%. The authors in [13] suggest a new method based on gray wolf optimization (GWO) and SVM. By this technique, they obtained 98.75% accuracy. In [14], a computer-aided system is implemented based on BWT and a genetic approach to assist radiologists. They attained a 92.3% accuracy and 0.93 dice similarity coefficient (DSC) value.

A study in [15] introduced a deep learning and DWT-based machine learning approach for detecting brain tumors. By this approach, they achieved 96.97% classification accuracy. In [16], a novel classification approach was developed based on a sine cosine algorithm (SCA) and local linear radial basis function neural network (LLRBFNN). Using

this, the authors obtained an accuracy of 97.76%. Work in [17] suggests an automatic brain tumor identification approach based on DWT and probabilistic neural networks (PNN). With this model, they attained 95% accuracy. In [18], developed an artificial intelligence technique based on fractal dimensions (FD) and particle swarm optimization (PSO). Therefore, the authors obtained 98.19% accuracy.

Work in [19] proposed a wavelet-energy and SVM classifier-based brain tumor classification approach. Through this, they attained 80.13% classification accuracy. A study in [20] developed an automatic methodology using a dilated convolutional neural network (D-CNN). Through this work, they achieved 96.82% accuracy. In [21], introduced a novel brain tumor diagnosis approach based on wavelet-entropy (WE) and naive Bayes (NB). Here, the authors achieved an accuracy of 92.6%.

In [22], proposed automatic brain tumor detection using a nonlinear normed residual-Markov random field (NLR-MRF), SVM, and multilayer perceptron (MLP). With this approach, they attained 0.77 DSC. the authors in [23] developed a novel approach to differentiate brain MR images based on curvelet and multi-SVM (M-SVM). As a result, the authors achieved 94.6% accuracy. A study in [24] proposed an unsupervised approach using a fuzzy K-means (FKM) based self-organizing map (SOM) algorithm. With this method, the authors attained 0.47 DSC.

Work in [25] presented a hybrid ensemble classification model for detecting MR-based brain tumors, and they attained 97.3% accuracy. In [26], a deep neural network (DNN) based brain tumor detection approach was developed, yielding 95.3% classification accuracy. The authors in [27] implemented an efficient brain tumor detection framework using DWT, a histogram of oriented gradients (HoG), and random forest (RF). Through this process, they obtained 98.37% accuracy. A study in [28] proposed a CNN model for identifying brain tumors from MR images and achieved approximately 89% accuracy.

In [29] presented an efficient methodology for discriminating brain MR images into healthy and pathological classes using the combination of various wavelets and an SVM learning approach. Based on this technique, the authors obtained 98% accuracy. Work in [30] suggested an intelligent design for identifying and classifying MR images using CNN, local binary patterns (LBP), and a multilayered SVM. Through these operations, they attained 99.3% accuracy. The authors in [31] present a new MR-based brain tumor classification methodology using CNN with transfer learning and PCA. With this process, they achieved 84% accuracy.

A study in [32] proposed a pre-trained CNN model such as VGG-16 with transfer learning to detect brain tumors automatically and yield 96% classification accuracy. In [33], a CNN-based detection approach was introduced to identify abnormal brain MR images and reached 97.78%



accuracy. In [34], the authors initiated an ensemble learning framework for classifying brain tumors using MR images and obtained 97.91% accuracy.

A. Research Gaps

The following points are to be observed from the conventional brain tumor identification and classification approaches:

1. Traditional local texture feature extraction approaches like LBP are sensitive to illumination variations, random noise, and rotations.

2. Most of the conventional methods utilize statistical texture features. However, these features do not provide the local texture information of region-of-interest (ROI) over brain MR images.

3. Few approaches have employed transform-based feature extraction techniques such as wavelets. Unfortunately, they perform poorly at the borders and textural regions of brain MR images.

4. A few models offer CNN-based brain tumor detection approaches requiring considerable data and high computational complexity.

5. Brain tumors (especially gliomas) are significantly infiltrated on imagery owing to fuzzy borders, and also very difficult to identify the tumor area.

B. Contributions

We proposed a new framework using shape and texture features to limit the above-mentioned issues. The significant contributions of the suggested model are as follows:

1. We introduce data augmentation using geometric transformation operators to improve the model's generalization ability.

2. We employed a modified pyramid histogram of gradients (MPHOG) and enhanced gradient LBP (EGLBP) to extract the inherent features of brain MR images. These features are robust to noise.

3. PROPOSED METHODOLOGY

Figure 1 shows the flow diagram of the suggested model for detecting brain tumors from MR images, and it includes four phases: preprocessing, segmentation, feature extraction, and classification.

A. Preprocessing

The preprocessing is twofold: First, we improve the contrast of an image and then perform data augmentation to enhance the accuracy of the proposed framework. In the following subsections, we discuss this in detail.

1) Contrast Enhancement

In the process of acquiring MR images, it may introduce unwanted information or artifacts. Therefore, radiologists

cannot extract or identify the affected area of the tumor completely. Hence, to avoid such a problem, we applied the median filter with a kernel size of 3×3 to enhance the contrast of brain MR images. The effect of preprocessing is shown in Figure 2 (e)-(h). After that, we employ image augmentation to increase the model's accuracy on the testing data by minimizing the overfitting problems.

2) Data Augmentation

In this work, to evaluate the performance of the proposed system, we acquired 160 T2-weighted brain MR images (20 normal and 140 abnormal) from the Harvard Medical School (HMS) open-access database (<https://www.med.harvard.edu/aanlib/>). However, these data need to be improved to develop an effective system. Therefore, we applied data augmentation using geometric operations such as rotation, scaling, translation, shearing, and reflection. Through this process, we attained 1260 abnormal and 180 normal images. The improved MR images of the brain are then segmented to locate the aberrant region.

B. Image Segmentation

Segmentation is a commonly used image processing method in several applications, such as medical imaging, content-based image retrieval, and computer and machine vision. It is crucial in the field of medical imaging, particularly during the diagnosis of people who suffer from brain tumors. In this work, the main idea behind this approach is to identify the tumor area (region of interest (ROI)) from brain MR images by identifying areas of normalcy and deviation. The thresholding and morphological operations can achieve this.

In our method, initially, we estimate the global thresholding (T) from the preprocessed brain MR images (P) using Otsu's thresholding [35] approach. Then, we separate the affected and unaffected regions using an estimated thresholding value. However, imperfections in the obtained threshold image occur with this process. Hence, to address this issue, we perform postprocessing using morphological operations [36], [37].

1) Otsu's thresholding

Otsu's thresholding [35] is a simple and frequently used automatic image thresholding technique. This approach yields a single gray-level thresholding value (T) that differentiates the pixels into tumor and non-tumor diagnoses, maximizing the between-class variance or minimizing the within-class variance. The results of Otsu's thresholding are illustrated in Figure 2 (i)-(l).

2) Postprocessing

Morphological operations are mainly used to eliminate the defects that occurred in Otsu's threshold image [See Figure 2 (i)-(l)] by taking into consideration the shape and boundary area of the tumor. Usually, to perform these operations, we require two elements, namely, the shape template (S) and threshold image (J). These operations can improve the effectiveness of detecting brain MR tumor

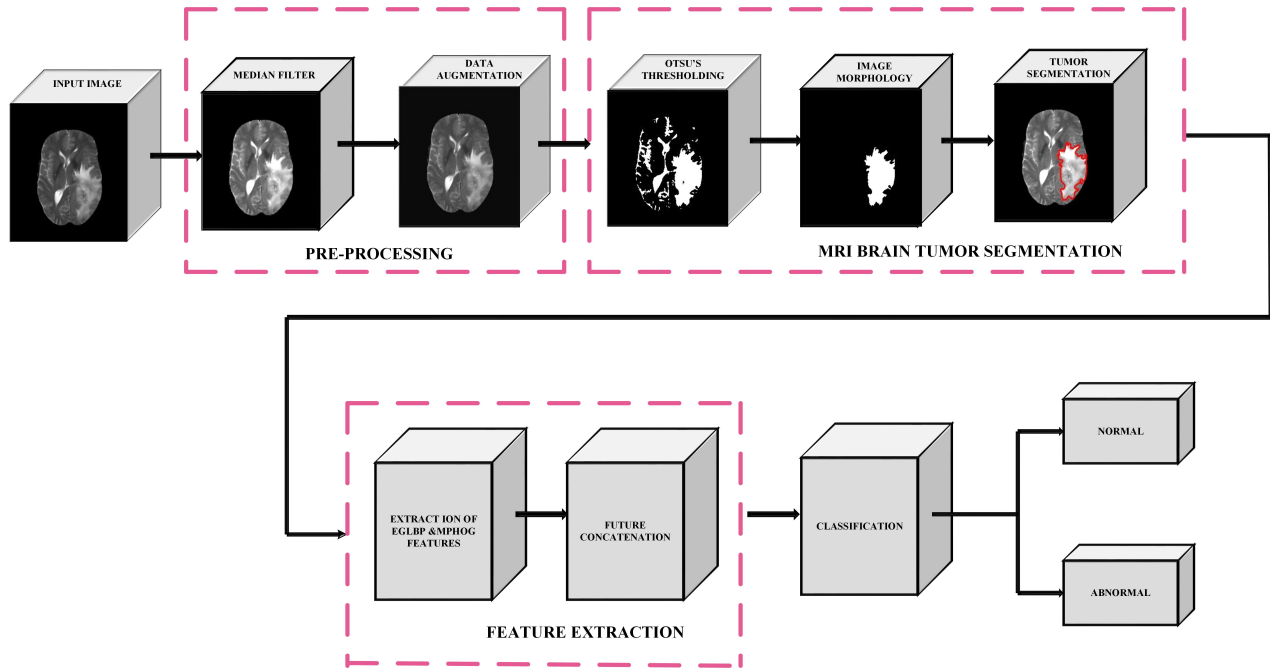


Figure 1. Block diagram of proposed brain tumor identification and classification approach

images. The outcomes of morphological operations are demonstrated in Figure 2 (m)-(p).

C. Feature Extraction

Feature extraction is essential in various fields, including computer vision, medical image processing, remote sensing, industrial automation, etc. Recently, researchers have developed numerous approaches [38]. Shape and texture are significant in medical image processing to distinguish brain MR images. We propose an MPHOG and EGLBP to meet this criterion. Using these methods, we can significantly capture the changes in the microstructures of brain MR images.

1) Enhanced Gradient LBP (EGLBP)

The LBP is an extensively used feature descriptor in medical image analysis since it captures the local variations in intensity due to tissue heterogeneity. Owing to this idea, in this study, we propose an enhanced gradient LBP (EGLBP), namely EGLBP1 and EGLBP2, motivated by the work suggested by the authors in [39]. In EGLBP1, we introduce a modified Prewitt kernel, whereas, in EGLBP2, we suggest a second derivative Sobel filter to estimate the gradient map (see Table 1). We establish the concept of rotation-invariant uniformity to efficiently capture the microstructures (lines, edges, and spots) that are present over brain MR images (riu2) into EGLBP ($EGLBP_{N,r}^{riu2}$).

To realize $EGLBP_{N,r}^{riu2}$; initially, we estimate the gradient magnitude using edge detection technique and then compute the LBP (LBP^{riu2}). The gradient magnitude (G) of an image can be evaluated by convolving the ROI of brain MR

image R with edge detection kernels (Sobel and Prewitt) as follows:

$$M(k) = \left((R(k) \odot E_x(k))^2 + (R(k) \odot E_y(k))^2 \right)^{1/2} \quad (1)$$

where ' \odot ' represents the convolution operator, E_x and E_y are the edge detection kernels along the x- and y-directions.

Thereafter, we determine the LBP^{riu2} for every pixel in the gradient magnitude map of the ROI using the following formulation

$$EGLBP_{N,r}^{riu2} = \begin{cases} \sum_{n=0}^{N-1} z(M_n - M_c), & U(EGLBP_{N,r}) \leq 2 \\ N + 1, & otherwise \end{cases} \quad (2)$$

Here, ' N ' denotes the size of the neighborhood; ' r ' represents the neighborhood radius; G_c and G_n are the gradient magnitudes at the center position and its corresponding neighbors; 'riu2' gives the rotation invariant uniform patterns with $U \leq 2$; $t(\cdot)$ denotes the thresholding function and is estimated using Eq.(3); U is the uniform criterion and is calculated by Eq.(4).

$$t(M_n - M_c) = \begin{cases} 1, & M_n \geq M_c \\ 0, & otherwise \end{cases} \quad (3)$$

$$U(EGLBP_{N,r}) = \|t(M_{N-1} - M_c) - t(M_0 - M_c)\| + \sum_{n=0}^{N-1} \|t(M_n - M_c) - t(M_{n-1} - M_c)\| \quad (4)$$

Hence, from Eq.(2), we conclude that $EGLBP_{N,r}^{riu2}$ has $N + 2$ local patterns. Using this, we efficiently capture the local

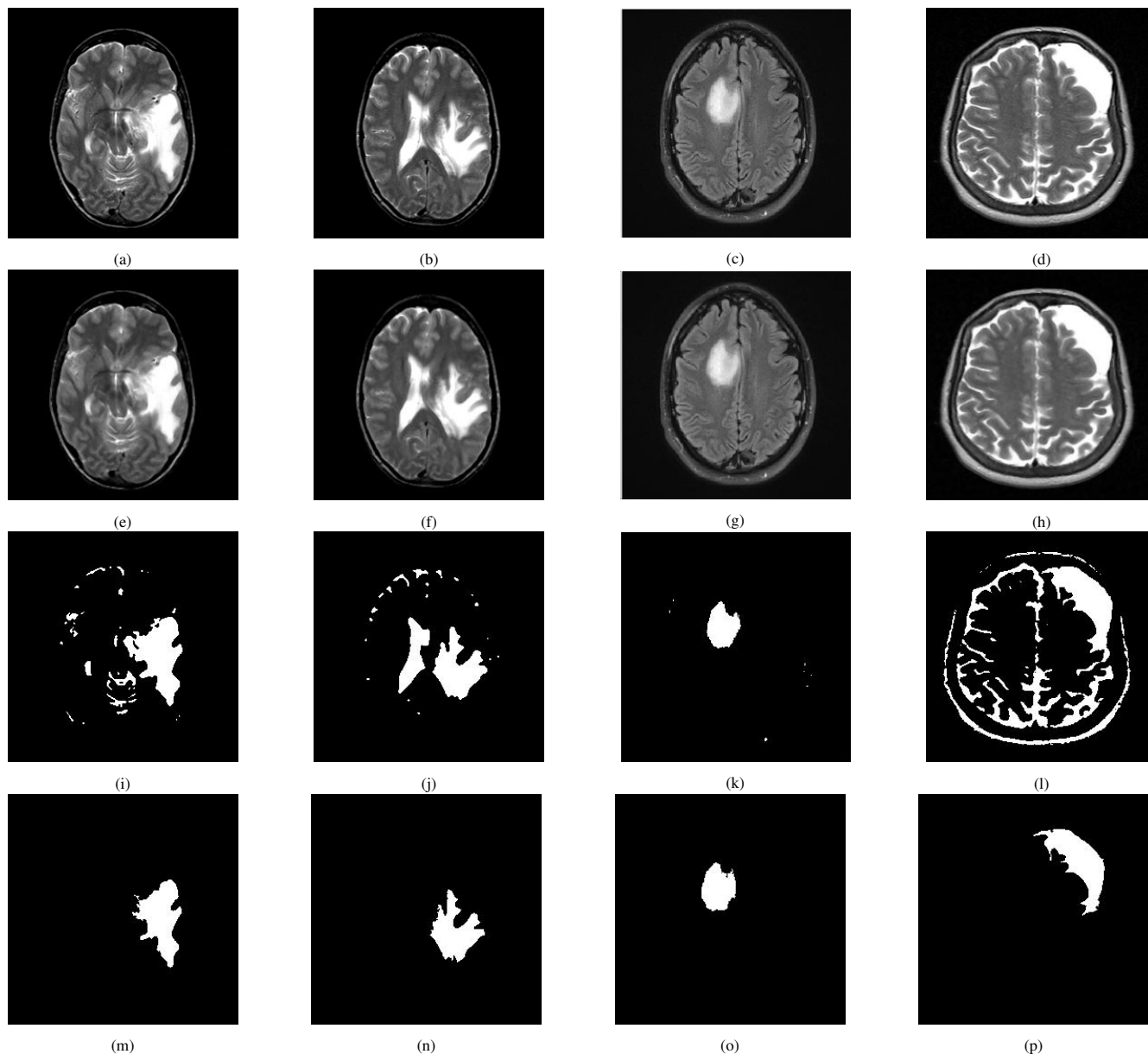


Figure 2. Outcomes of the suggested segmentation technique: (a)-(d) Input images; (e)-(h) Enhanced images; (i)-(l) Segmented images; (m)-(p) Refined segmented images.

gradient patterns of the ROI, namely the microstructures at distinct locations.

To illustrate local gradient patterns, $EGLBP_{N,r}^{riu2}$ encoded only signs of the difference between pixels located at the center position and corresponding neighbors. However, it omits the gradient magnitude of the difference. With this concern, we cannot separate the weak contrast local gradient patterns from strong ones. To overcome this issue, we aggregate the gradient magnitudes of pixels with the same $EGLBP_{N,r}^{riu2}$ pattern, which is called the histogram of gradient magnitude-weighted EGLBP (GMWH-EGLBP)

and is given by

$$h_{EGLBP}(l) = \sum_{k=1}^K w_k f(EGLBP_{N,r}^{riu2}(l, k)) \quad (5)$$

where ‘K’ is the number of pixels, ‘l’ denotes the possible EGLBP patterns, and ‘w’ represents the weights associated with EGLBP. Hence, from Eq. (5), we concluded that our suggested approach captures both structural and contrast information of microstructures over ROIs. Here, to estimate, $EGLBP_{N,r}^{riu2}$ we consider $N = 8$ and $r = 1$. With this, we attained ten structural features from each EGLBP. The

TABLE I. Modified Prewitt and second derivative Sobel edge detection kernels

Kernel	E_x	E_y
Prewitt	$\begin{bmatrix} -2 & -1 & 0 & 1 & 2 \\ -2 & -4 & 0 & 2 & 4 \\ -2 & -4 & 0 & 2 & 4 \\ -2 & -4 & 0 & 2 & 4 \\ -2 & -1 & 0 & 1 & 2 \end{bmatrix}$	E_x^{tr}
Sobel	$\begin{bmatrix} 1 & 4 & 6 & 4 & 1 \\ 0 & 0 & 0 & 0 & 0 \\ -2 & -8 & -12 & -8 & -2 \\ 0 & 0 & 0 & 0 & 0 \\ 1 & 4 & 6 & 4 & 1 \end{bmatrix}$	E_y^{tr}

whole process of extracting local texture features using $EGLBP_{N,r}^{riu2}$ is shown in Figure 3.

2) Modified Pyramid Histogram of Oriented Gradients (MPHOG)

Feature extraction is essential in various fields, including LBP efficiently providing the local texture details about the ROI of brain MR images; however, in the classification scenario, shape information also plays a prominent role in enhancing the diagnosis performance. We adopted a pyramid histogram of oriented gradients (PHOG) [40] local feature descriptor to extract such shape information. Unlike other descriptors, [41], the PHOG is evaluated on sub-regions of the image or a fine grid of uniform cells. To implement PHOG, they utilized the canny edge detection approach to estimate edge orientations. However, the canny edge detection technique makes it very difficult to identify the edges, particularly if the image is blurred [42]. To address this problem, we introduce fuzzy logic-based edge detection [43] into PHOG, known as MPHOG.

The MPHOG descriptor locally illustrates the shape and spatial details of the ROI. The frequency distributions of gray levels of edge orientations over sub-regions describe the local shape. From this, we observed that MPHOG describes both edge location and direction. Similarly, the spatial details are characterized by tiling the image into regions at various resolutions using spatial pyramid matching [44]. Here, initially, we subdivide an ROI of a brain MR image into L -cells at different resolutions by doubling the number of subdivisions at each pyramid level. Then we compute the HOG over each cell and concatenate them into a single feature vector.

To construct MPHOG, at the first level, we split the image into 2^l cells about the direction of each axis. Consequently, level 0 is represented by an M -vector correspondence to the M -bins of histograms; level 1 is illustrated by $4M$ -vectors, and so on. Therefore, for an entire image, the MPHOG is represented by

$$M \times \sum_{l \in L} 4^l \quad (6)$$

Hence, from Eq. (9), we conclude that the MPHOG provides the spatial details of an ROI. In this work, to obtain the MPHOG, we chose $M=8$ and $L=2$. Therefore, the total length of MPHOG is $8 \times (1+4+16) = 21 \times 8 = 168$. The corresponding histogram features of the MPHOG are represented in Figure 4. After that, a method known as serial fusion is used to concatenate the previously retrieved features.

3) Feature Concatenation

To increase the accuracy of the classifier, we concatenate the features of EGLBP1 (α), EGLBP2 (β), and MPHOG (ζ) into a single vector (f) by a simple serial concatenation approach. The corresponding concatenated feature vector is given by

$$f_s = [\gamma, \beta, \zeta] \quad (7)$$

With this concatenation, finally, from each ROI of the brain MR image, we obtained 188 features with dimensions of 1×188 . The entire process of concatenation is described in Figure 5. Afterward, the concatenated feature vector is fed to the classifier to distinguish between normal and abnormal.

D. Classification

Classification is one of the critical aspects in clinical applications to avoid incorrect predictions while interpreting brain MR images. There are several approaches to categorizing these images. Among them, we utilized one of the famous and widely used supervised machine learning approaches, namely support vector machine (SVM) [45], K-nearest neighbors (KNN) [46], and LogitBoost ensemble learning (LBEL) [47]

1) Support Vector Machines (SVM)

The SVM [45] is a frequently used learning strategy for analyzing classification problems, particularly binary or binomial classification. To distinguish the data points within the classes, SVM estimates an optimal hyperplane by maximizing the margin between the data points and the decision surface. In this work, we have chosen a radial basis function (RBF) with default parameters for binomial classification because:

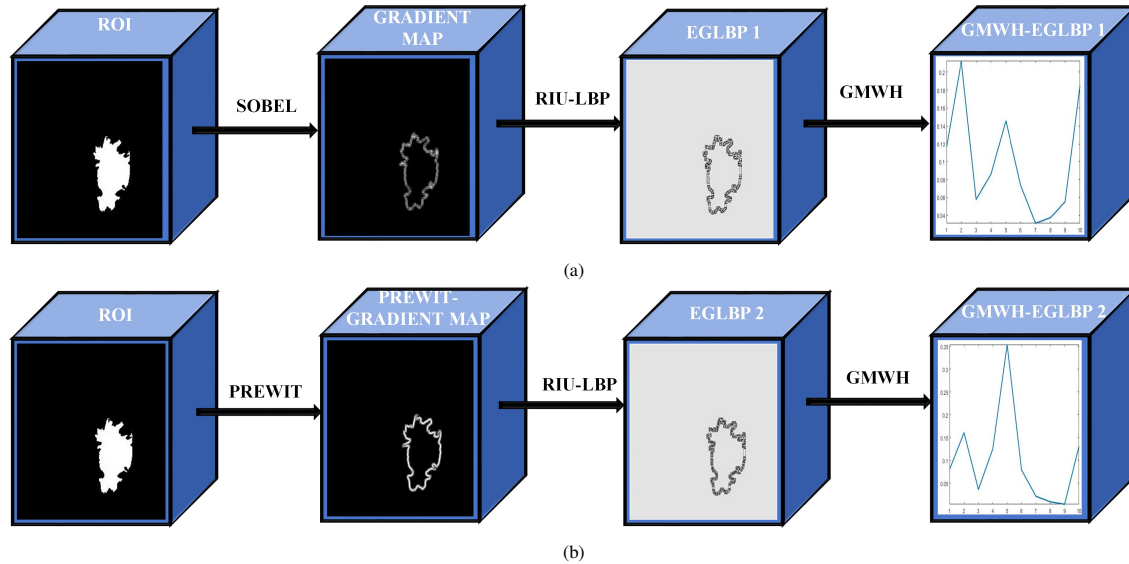


Figure 3. Illustration of EGLBPs (a) EGLBP1; (b) EGLBP2.

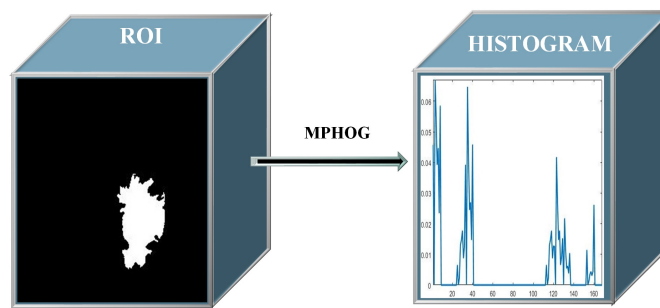


Figure 4. Illustration of Histogram Features of MPHOG

1. It provides good performance when the feature set contains fewer features.

2. The RBF kernel needs fewer hyperparameters.

The following equation defines the RBF kernel

$$F(y_i, y_j) = \exp(-\alpha \|y_i - y_j\|^2), \alpha > 0 \quad (8)$$

where y_i , and y_j denotes the objects i and j ; α denotes the kernel variable, and it is used to evaluate the smoothness of the boundary between the classes in the original object space.

2) K-Nearest Neighbors (KNN)

KNN [46] is widely utilized as a supervised learning tool for studying classification and regression issues. However, its primary application is in the realm of classification issues. The KNN stores all data points of corresponding classes and then categorizes the new classes based on the distance metric. Generally, in KNN, the classes are separated by a majority vote of their neighbors. Based on its majority vote, the KNN predicts more classes among those

based on a distance measure. In this work, we considered Euclidean distance, and the number of neighbors K is 3.

3) LogitBoost Ensemble Learning (LBEL)

Ensemble learning is a typical and widely used approach in statistics and machine learning applications. The main objective of ensemble learning is to enhance the predictive performance of machine learning by composing several trees; we utilized LogitBoost ensemble learning [47] since it effectively reduces bias and variance. With this, we can improve the performance of binomial or binary classification problems.

Let us say that the input vector $x = [x_1, x_2, x_3, \dots, x_k]$ with k factors, and $y = [0, 1]$ be the output indicates normal and abnormal classes. Based on the following formula, the LogitBoost method makes an ensemble learning model:

$$h^{(n)} = \operatorname{argmin}_h \sum_{s=1}^k w_s^{(n)} (r_s^{(n)} - h(x_j))^2 \quad (9)$$

where n is the number of decision trees, h is the classifier, and r and w are the working responses and weights,

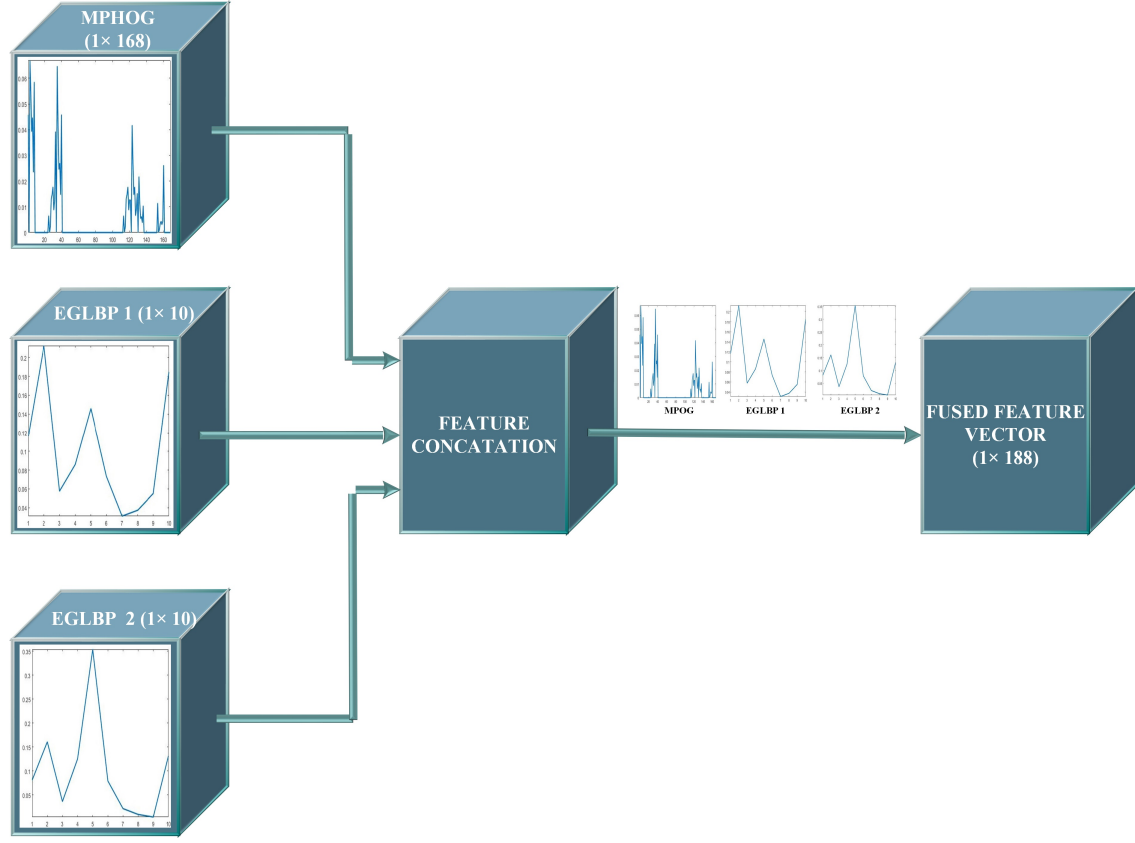


Figure 5. Illustration of Feature Concatenation

respectively, determined by the equations above:

$$w_s^{(n)} = q^{(n-1)} (1 - q^{(n-1)}) \quad (10)$$

$$w_s^{(n)} = \frac{y_s - q^{(n-1)}(x_s)}{h^{(n-1)} (1 - q^{(n-1)})} \quad (11)$$

where $q(x_s)$ is an estimate of the likelihood of belonging to either the normal or abnormal class. Then, using Eq.(10) and Eq.(11), $H^{(n)}$ is the improved ensemble learning model, $q^{(n-1)}$ is the corresponding probabilities of classes,

$$H^{(n)}(x_s) = H^{(n-1)}(x_s) + \frac{1}{2}h^{(n)}(x_s) \quad (12)$$

$$w_j^{(n)} = \frac{y_s - q^{(n-1)}(x_s)}{q^{(d-1)} (1 - q^{(n-1)})} \quad (13)$$

Finally, after all the updates have been made, use the following criteria to determine whether the MR pictures of the brain are normal or aberrant.

$$sign[H^{(n)}(x_s)]_{s=1 \rightarrow k, d=1 \rightarrow 100} = \begin{cases} 1(Abnormal), & H^n(x_s) < 0 \\ 0(Normal), & H^n(x_s) \geq 0 \end{cases} \quad (14)$$

The efficacy of the LBEL strategy is contingent on the classifier or a selection of learners. In this work, we consider the decision stump tree learning technique to construct an

ensemble learning model due to its ease of use and deliver a competitive result with boosting. For better classification, we have chosen 100 decision-tree stump learners to train in the LBEL approach in this study.

E. Metrics

To analyze the performance of the implemented strategy, we consider the following measures [48]:

$$Accuracy = \frac{TP + TN}{TP + TN + FP + FN} \quad (15)$$

$$True\ Positive\ Rate\ (TPR) = \frac{TP}{TP + FN} \quad (16)$$

$$True\ Negative\ Rate\ (TNR) = \frac{TN}{TN + FP} \quad (17)$$

$$Positive\ Predicted\ Value\ (PPV) = \frac{TP}{TP + FP} \quad (18)$$

$$F\text{-Score} = 2 \left(\frac{PPV \times TPR}{PPV + TPR} \right) \quad (19)$$

$$Dice\ similarity\ score\ (DSC) = \frac{2 \times |T \cap T_G|}{|T| + |T_G|} \quad (20)$$

$$Area\ Under\ Curve\ (AUC) = \frac{TPR + TNR}{2} \quad (21)$$



where T , T_G , TN , FN , FP , and TN are segmented image, ground truth, true positive, false negative, false positive, and true negative, respectively.

4. RESULTS AND DISCUSSIONS

This paper introduced a distinctive methodology for recognizing and discriminating brain MR images using feature descriptors such as EGLBP and MPHOG. Here, primarily, we improve the brightness of brain MR images by the median filter. We identified the infected tumor region (ROI) using Otsu's thresholding and morphological operations. Furthermore, to categorize brain MR images, we extracted significant textures and shaped informative features locally using EGLBP and MPHOG. To enhance the detection accuracy, we concatenate the resultant features serially. Finally, we categorized brain MRI images as normal or abnormal using supervised ML approaches such as SVM, KNN, DT, and ensemble learning. The experimental results are split into two subsections for a better understanding: 1. Segmentation; 2. Classification

A. Segmentation Analysis

The evaluation of the presented segmentation on the HMS database is depicted in Table 2. At the same time, the assessment of the presented technique with state-of-the-art approaches is represented in Table 3. This process achieved 0.86 DSC, 98.86% PPV, 98.93% TPR, 98.67% F-score, 88.89% TNR, 93.91% AUC, and 97.96% accuracy (see Table 2). Table 3 shows that the presented segmentation framework achieved accuracy compared to well-received approaches. Note that higher values of TPR, TNR, DSC, F-measure, PPV, and accuracy illustrate better performance in the segmentation assessment. A slight increase in these parameters is crucial for a radiologist or physician.

B. Classification Analysis

The classification outcomes of the proposed approach are represented in Table 4, and their ROC curves are depicted in Figure 6. From there, we observed that the SVM performs better than other supervised learning methods with 100% TPR, 93.89% TNR, 99.13% PPV, 96.82% AUC, and 99.24% accuracy when it is used EGLBP+MPHOG features. Therefore, from these experimental results, we conclude that in comparison with other features, by fused features (EGLBP+MPHOG), we effectively categorized MR-based brain images. The proposed classification experimental outcomes are compared with well-received strategies (see Table 5). Based on these experiments, we noted that the proposed technique attained good accuracy compared to existing methods. From the analysis of classification and segmentation outcomes, we summarize the merits and demerits of the implemented framework:

1. By the EGLBP features, we cannot classify the brain MR images effectively since they neglect the features of nonuniform pixels. Due to this, we may lose some details of two corners' adjacent pixels.

2. Using MPHOG features, we achieved good results compared to EGLBPs, but inferior results to EGLBPs+MPHOG features because it will not significantly categorize the tumors, which will have high similarity.

3. By EGLBPs+ MPHOG features, we obtained better accuracy than other features since they effectively captured the gradient, local texture, spatial, and shape informative features.

4. Compared with existing methodologies, ensemble learning performs better when implementing EGLBPs+MPHOG features.

5. The suggested segmentation approach outperformed other current systems in terms of DSC, recall, and accuracy because it successfully distinguishes between the infected and the non-infected area (see Figure 2 (m)-(p)).



TABLE II. Performance of the proposed segmentation approach

Image	DSC	PPV	TPR	TNR	F-Score	AUC	Accuracy
1	90.49	99.64	99.55	99.55	99.59	99.55	99.22
2	80.47	95.74	99.82	68.17	97.74	84	95.95
3	72.56	92.77	99.66	57.98	96.08	78.82	93.15
4	91.39	99.64	99.41	93.27	99.52	96.34	99.10
5	85.53	99.89	99.34	95.35	99.61	97.35	99.25
6	76.71	99.78	97.45	95.56	98.6	96.51	97.36
7	89.49	99.71	99.25	93.86	99.47	96.55	99
8	87.73	99.81	99.19	95.05	99.5	97.12	99.04
9	91.24	98.34	98.64	90.54	98.47	94.57	97.40
10	90.89	99.34	98.34	94.66	98.84	96.50	97.94
11	81.55	99.59	96.98	95.02	98.27	96	96.84
12	89.94	99.71	98.91	95.33	99.30	97.22	98.7
13	85.36	99.35	97.65	93.16	98.49	95.4	97.26
14	85.08	97.87	98.91	81.13	98.38	90.02	97.09
15	87.93	98.81	99.42	84.38	95.11	91.90	98.35
16	86.69	99.83	99.42	93.4	99.62	96.41	99.27
17	89.19	99.82	98.79	97.03	99.3	97.91	98.70
18	85.90	99.53	98.91	91.01	99.22	94.96	98.52
19	85.33	99.14	100	74.42	99.57	87.21	99.07
Average	85.98	98.86	98.93	88.89	98.67	93.91	97.96

TABLE III. Comparative analysis of the suggested and existing brain tumor segmentation models.

Year	Technique	DSC
2016	SOM-FKM [24]	0.47
2017	BWT-SVM [5]	0.82
2019	NLR-MRF [22]	0.77
	The Proposed	0.86

TABLE IV. Classification performance of the suggested framework

Feature	Learning Approach	TPR	TNR	PPV	F-Score	AUC	Accuracy
ELGBP	SVM	99.92	66.67	95.45	97.63	83.29	95.76
	KNN	97.78	75	96.47	98.477	86.39	94.93
	LBEL	99.76	85	97.89	98.81	92.38	97.92
MPHOG	SVM	99.44	84.44	97.81	98.62	91.94	97.57
	KNN	99.68	87.78	98.27	98.97	93.73	98.19
	LBEL	99.28	90	98.58	98.43	94.64	98.12
ELGBP+MPHOG	SVM	100	93.89	99.13	99.56	96.94	99.24
	KNN	99.76	93.89	99.13	99.44	96.82	99.03
	LBEL	99.6	90.55	98.66	99.12	95.07	98.47

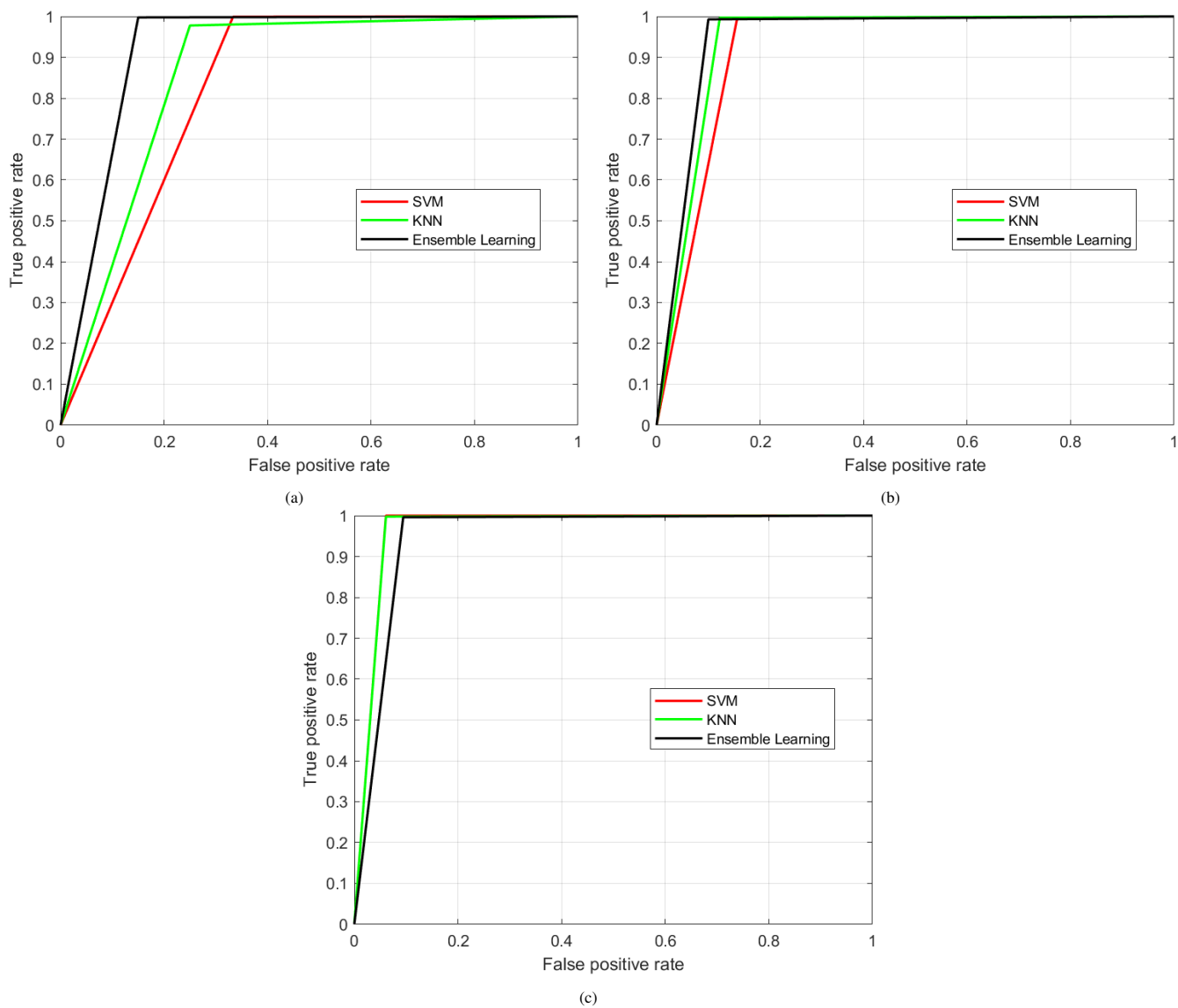


Figure 6. Receiver Operating Characteristics (ROC) (a) EGLBP; (b) MPHOG; (c) EGLBP+MPHOG.



TABLE V. Comparison of classification performance of the proposed and existing frameworks

Year	Technique	Accuracy
2006	DWT+SVM [7]	97.15
2010	DWT+PCA+KNN [11]	97.54
2011	DWT + PCA + BPNN [6]	98.29
2015	WE+SVM [19]	80.13
2015	WE+NB [21]	91.87
2016	FRFE+MLP [10]	97.81
2016	FD+ PSO [18]	98.19
2017	DWT+ELM [12]	98.33
2018	HMI+SLN [4]	98.25
2018	TBRO-MPKDD [8]	96.57
2018	WE-Kernel ELM [9]	98.38
2018	DWT-DNN [15]	96.97
2018	DWT-PNN [17]	95
2019	Watershed-SVM [3]	98.17
2019	SCA+LLRBFNN [16]	97.76
2020	Dilated CNN [20]	96.82
2020	M-SVM [23]	94.6
2021	Hybrid Ensemble Classifier [25]	97.3
2021	DNN [26]	95.3
2021	DWT+HOG+RF [27]	98.37
2021	CNN [28]	89
2021	DWT+SVM [29]	98
2022	PCA+CNN [31]	84
2022	VGG-16 [32]	96
2022	CNN [33]	97.78
2022	Ensemble Learning [34]	97.91
	The Proposed (EGLBP+MPHOG+SVM)	99.3



5. CONCLUSION AND FUTURE SCOPE

In this work, we proposed a novel approach for identifying and distinguishing brain MR images. The proposed method initially used a median filter to enhance the contrast of brain MR images. Then, data augmentation was employed to improve the model's generalization ability. Subsequently, obtain the ROI using thresholding and a morphological-based segmentation process. Later, the extracted ROI is fed to the feature extraction procedure to attain the significant local texture and shape informative features. We constructed a feature vector to enhance the classification performance by concatenating the features. Finally, to discriminate the brain MR images, the resultant feature vector is fed to supervised learning models. From the detailed analysis of classification results, the SVM learning approach gives better results than other classifiers. Similarly, from the segmentation outcomes, we noted that the suggested detection process successfully identified the whole tumor region of the brain MR image. Therefore, from these investigations, we observed that the presented framework could be employed as a predictive tool, particularly at earlier stages. Our work will extend to other medical diagnosis applications such as skin, breast, and lung cancers. In addition, we extend to multiclass classification.

REFERENCES

- [1] A. Tiwari, S. Srivastava, and M. Pant, "Brain tumor segmentation and classification from magnetic resonance images: Review of selected methods from 2014 to 2019," *Pattern Recognition Letters*, vol. 131, pp. 244–260, 2020.
- [2] H. Kasban, M. El-Bendary, and D. Salama, "A comparative study of medical imaging techniques," *International Journal of Information Science and Intelligent System*, vol. 4, no. 2, pp. 37–58, 2015.
- [3] M. A. Khan, I. U. Lali, A. Rehman, M. Ishaq, M. Sharif, T. Saba, S. Zahoor, and T. Akram, "Brain tumor detection and classification: A framework of marker-based watershed algorithm and multilevel priority features selection," *Microscopy research and technique*, vol. 82, no. 6, pp. 909–922, 2019.
- [4] H. Wang, Y. Lv, H. Chen, Y. Li, Y. Zhang, and Z. Lu, "Smart pathological brain detection system by predator-prey particle swarm optimization and single-hidden layer neural-network," *Multimedia Tools and Applications*, vol. 77, no. 3, pp. 3871–3885, 2018.
- [5] N. B. Bahadure, A. K. Ray, and H. P. Thethi, "Image analysis for mri based brain tumor detection and feature extraction using biologically inspired bwt and svm," *International journal of biomedical imaging*, vol. 2017, 2017.
- [6] Y. Zhang, Z. Dong, L. Wu, and S. Wang, "A hybrid method for mri brain image classification," *Expert Systems with Applications*, vol. 38, no. 8, pp. 10049–10053, 2011.
- [7] S. Chaplot, L. M. Patnaik, and N. R. Jagannathan, "Classification of magnetic resonance brain images using wavelets as input to support vector machine and neural network," *Biomedical signal processing and control*, vol. 1, no. 1, pp. 86–92, 2006.
- [8] P. Kanmani and P. Marikkannu, "Mri brain images classification: a multi-level threshold based region optimization technique," *Journal of medical systems*, vol. 42, no. 4, pp. 1–12, 2018.
- [9] S. Lu, Z. Lu, J. Yang, M. Yang, and S. Wang, "A pathological brain detection system based on kernel based elm," *Multimedia tools and applications*, vol. 77, no. 3, pp. 3715–3728, 2018.
- [10] Y. Zhang, Y. Sun, P. Phillips, G. Liu, X. Zhou, and S. Wang, "A multilayer perceptron based smart pathological brain detection system by fractional fourier entropy," *Journal of medical systems*, vol. 40, no. 7, pp. 1–11, 2016.
- [11] E.-S. A. El-Dahshan, T. Hosny, and A.-B. M. Salem, "Hybrid intelligent techniques for mri brain images classification," *Digital signal processing*, vol. 20, no. 2, pp. 433–441, 2010.
- [12] S. Lu, X. Qiu, J. Shi, N. Li, Z.-H. Lu, P. Chen, M.-M. Yang, F.-Y. Liu, W.-J. Jia, and Y. Zhang, "A pathological brain detection system based on extreme learning machine optimized by bat algorithm," *CNS & Neurological Disorders-Drug Targets (Formerly Current Drug Targets-CNS & Neurological Disorders)*, vol. 16, no. 1, pp. 23–29, 2017.
- [13] H. M. Ahmed, B. A. Youssef, A. S. Elkorany, Z. F. Elsharkawy, A. A. Saleeb, and F. A. El-Samie, "Hybridized classification approach for magnetic resonance brain images using gray wolf optimizer and support vector machine," *Multimedia Tools and Applications*, vol. 78, no. 19, pp. 27983–28002, 2019.
- [14] N. B. Bahadure, A. K. Ray, and H. P. Thethi, "Comparative approach of mri-based brain tumor segmentation and classification using genetic algorithm," *Journal of digital imaging*, vol. 31, no. 4, pp. 477–489, 2018.
- [15] H. Mohsen, E.-S. A. El-Dahshan, E.-S. M. El-Horbaty, and A.-B. M. Salem, "Classification using deep learning neural networks for brain tumors," *Future Computing and Informatics Journal*, vol. 3, no. 1, pp. 68–71, 2018.
- [16] S. Mishra, P. Sahu, and M. R. Senapati, "Masca-pso based llrbfn model and improved fast and robust fcm algorithm for detection and classification of brain tumor from mr image," *Evolutionary Intelligence*, vol. 12, no. 4, pp. 647–663, 2019.
- [17] N. Varuna Shree and T. Kumar, "Identification and classification of brain tumor mri images with feature extraction using dwt and probabilistic neural network," *Brain informatics*, vol. 5, no. 1, pp. 23–30, 2018.
- [18] Y.-D. Zhang, X.-Q. Chen, T.-M. Zhan, Z.-Q. Jiao, Y. Sun, Z.-M. Chen, Y. Yao, L.-T. Fang, Y.-D. Lv, and S.-H. Wang, "Fractal dimension estimation for developing pathological brain detection system based on minkowski-bouligand method," *IEEE Access*, vol. 4, pp. 5937–5947, 2016.
- [19] G. Zhang, Q. Wang, C. Feng, E. Lee, G. Ji, S. Wang, Y. Zhang, and J. Yan, "Automated classification of brain mr images using wavelet-energy and support vector machines," in *2015 International conference on mechatronics, electronic, industrial and control engineering (MEIC-15)*. Atlantis Press, 2015, pp. 683–686.
- [20] S. S. Roy, N. Rodrigues, and Y. Taguchi, "Incremental dilations using cnn for brain tumor classification," *Applied Sciences*, vol. 10, no. 14, p. 4915, 2020.
- [21] X. Zhou, S. Wang, W. Xu, G. Ji, P. Phillips, P. Sun, and Y. Zhang, "Detection of pathological brain in mri scanning based on wavelet-entropy and naive bayes classifier," in *International conference on bioinformatics and biomedical engineering*. Springer, 2015, pp. 201–209.



- [22] Y. Kurmi and V. Chaurasia, "Classification of magnetic resonance images for brain tumour detection," *IET Image Processing*, vol. 14, no. 12, pp. 2808–2818, 2020.
- [23] U. N. Hussain, M. A. Khan, I. U. Lali, K. Javed, I. Ashraf, J. Tariq, H. Ali, and A. Din, "A unified design of aco and skewness based brain tumor segmentation and classification from mri scans," *Journal of Control Engineering and Applied Informatics*, vol. 22, no. 2, pp. 43–55, 2020.
- [24] G. Vishnuvarthanan, M. P. Rajasekaran, P. Subbaraj, and A. Vishnuvarthanan, "An unsupervised learning method with a clustering approach for tumor identification and tissue segmentation in magnetic resonance brain images," *Applied Soft Computing*, vol. 38, pp. 190–212, 2016.
- [25] G. Garg and R. Garg, "Brain tumor detection and classification based on hybrid ensemble classifier," *arXiv preprint arXiv:2101.00216*, 2021.
- [26] M. B. Sahaai et al., "Brain tumor detection using dnn algorithm," *Turkish Journal of Computer and Mathematics Education (TURCOMAT)*, vol. 12, no. 11, pp. 3338–3345, 2021.
- [27] M. Thayumanavan and A. Ramasamy, "An efficient approach for brain tumor detection and segmentation in mr brain images using random forest classifier," *Concurrent Engineering*, vol. 29, no. 3, pp. 266–274, 2021.
- [28] P. G. Brindha, M. Kavinraj, P. Manivasakam, and P. Prasanth, "Brain tumor detection from mri images using deep learning techniques," in *IOP Conference Series: Materials Science and Engineering*, vol. 1055, no. 1. IOP Publishing, 2021, p. 012115.
- [29] S. K. Mishra and V. H. Deepthi, "Brain image classification by the combination of different wavelet transforms and support vector machine classification," *Journal of Ambient Intelligence and Humanized Computing*, vol. 12, no. 6, pp. 6741–6749, 2021.
- [30] M. Kolla, R. K. Mishra, S. Zahoor ul Huq, Y. Vijayalata, M. V. Gopalachari, and K.-e.-A. Siddiquee, "Cnn-based brain tumor detection model using local binary pattern and multilayered svm classifier," *Computational Intelligence and Neuroscience*, vol. 2022, 2022.
- [31] P. Modiya and S. Vahora, "Brain tumor detection using transfer learning with dimensionality reduction method," *International Journal of Intelligent Systems and Applications in Engineering*, vol. 10, no. 2, pp. 201–206, 2022.
- [32] C. Srinivas, N. P. KS, M. Zakariah, Y. A. Alothaibi, K. Shaukat, B. Partibane, and H. Awal, "Deep transfer learning approaches in performance analysis of brain tumor classification using mri images," *Journal of Healthcare Engineering*, vol. 2022, 2022.
- [33] S. Feshawy, W. Saad, M. Shokair, and M. Dessouky, "Proposed approaches for brain tumors detection techniques using convolutional neural networks," *International Journal of Telecommunications*, vol. 2, no. 01, pp. 1–14, 2022.
- [34] R. Kaur, A. Doegar, and G. K. Upadhyaya, "An ensemble learning approach for brain tumor classification using mri," in *Soft Computing: Theories and Applications*. Springer, 2022, pp. 645–656.
- [35] N. Otsu, "A threshold selection method from gray-level histograms," *IEEE transactions on systems, man, and cybernetics*, vol. 9, no. 1, pp. 62–66, 1979.
- [36] R. C. Gonzalez, S. L. Eddins, and R. E. Woods, *Digital image publishing using MATLAB*. Prentice Hall, 2004.
- [37] L. Vincent, "Morphological grayscale reconstruction in image analysis: applications and efficient algorithms," *IEEE transactions on image processing*, vol. 2, no. 2, pp. 176–201, 1993.
- [38] A. Humeau-Heurtier, "Texture feature extraction methods: A survey," *IEEE access*, vol. 7, pp. 8975–9000, 2019.
- [39] Q. Li, W. Lin, and Y. Fang, "No-reference quality assessment for multiply-distorted images in gradient domain," *IEEE Signal Processing Letters*, vol. 23, no. 4, pp. 541–545, 2016.
- [40] A. Bosch, A. Zisserman, and X. Munoz, "Representing shape with a spatial pyramid kernel," in *Proceedings of the 6th ACM international conference on Image and video retrieval*, 2007, pp. 401–408.
- [41] C. Leng, H. Zhang, B. Li, G. Cai, Z. Pei, and L. He, "Local feature descriptor for image matching: A survey," *IEEE Access*, vol. 7, pp. 6424–6434, 2018.
- [42] R. Maini and H. Aggarwal, "Study and comparison of various image edge detection techniques," *International journal of image processing (IJIP)*, vol. 3, no. 1, pp. 1–11, 2009.
- [43] E. K. Kaur, V. Mutenja, and I. S. Gill, "Fuzzy logic based image edge detection algorithm in matlab," *International Journal of Computer Applications*, vol. 1, no. 22, pp. 55–58, 2010.
- [44] K. Grauman and T. Darrell, "The pyramid match kernel: Discriminative classification with sets of image features," in *Tenth IEEE International Conference on Computer Vision (ICCV'05) Volume 1*, vol. 2. IEEE, 2005, pp. 1458–1465.
- [45] V. Vapnik, *The nature of statistical learning theory*. Springer science & business media, 1999.
- [46] P. Cunningham and S. J. Delany, "K-nearest neighbour classifiers-a tutorial," *ACM Computing Surveys (CSUR)*, vol. 54, no. 6, pp. 1–25, 2021.
- [47] J. Friedman, T. Hastie, and R. Tibshirani, "Additive logistic regression: a statistical view of boosting (with discussion and a rejoinder by the authors)," *The annals of statistics*, vol. 28, no. 2, pp. 337–407, 2000.
- [48] K. R. Reddy and R. Dhuli, "Segmentation and classification of brain tumors from mri images based on adaptive mechanisms and eldp feature descriptor," *Biomedical Signal Processing and Control*, vol. 76, p. 103704, 2022.



Dr.K.Sowjanya is an Assistant Professor in the Department of Electronics and Communication Engineering, KITS, Warangal, Telangana State, India. She has publications in reputed international journals and presented her research at national and international conferences. She is a member of IEEE and IETE. She has also authored two books. She also reviews the International Journal

of Engineering and Technology Innovation (IJETI) and IET Image Processing. Her research interests are Artificial Intelligence (AI), Swarm Intelligence, Machine learning (ML), Meta-heuristics, and Engineering Optimization.



K. Rasool Reddy received his B.E degree in Electronics and Communication Engineering from Sir C.R. Reddy College of Engineering, Andhra Pradesh, India, in 2011 and M.Tech from JNTU Hyderabad, India, in 2013. Since 2018, he has been pursuing a Ph.D. in the School of Electronics Engineering at Vellore Institute of Technology-Andhra Pradesh (VIT-AP) university, India. His research interests include Biomedical

image processing, Computer vision, Machine learning, and Deep learning.



Merugu Raveena is a student in the Department of Electronics and Communication Engineering, KITS, Warangal, Telangana State, India.